Morphological changes of wide polyoxymethylene rod during a microwave heating drawing process

Y. Takeuchi, K. Nakagawa and F. Yamamoto
NTT Ibaraki Electrical Communication Laboratories, Tokai, Ibaraki 319-11, Japan
(Received 15 April 1985; revised 7 June 1985)

The microwave heating drawing process for producing a polyoxymethylene (POM) rod (2.5 mm in diameter) with a sonic modulus of ~40 GPa has been analysed by investigating the changes in both orientation and thermal properties during drawing. During the initial crystalline deformation in the necking region, the lamellae are oriented perpendicular to the draw direction and are then unfolded into microfibrils. The crystalline orientation function reaches a high value (0.988) at a draw ratio of 6 immediately after necking. In the advanced ultra-drawing stage, the Young modulus increases gradually with increasing amorphous orientation. At the same time, the orientation distribution in the radial direction is caused by the temperature distribution induced in the radial direction of the rod. It is noted that fine adjustments of ambient temperature and microwave power are required to get ultra-high-modulus POM rods over 40 GPa with large cross-sections.

(Keywords: polyoxymethylene; microwave heating; drawing process; necking; orientation distribution)

INTRODUCTION

Ultra-high-modulus polyoxymethylene (POM) with a Young modulus of ~60 GPa can be made by the microwave selective absorption heating drawing (MISELA) method[1]. The MISELA method is suitable for drawing POM rods, tapes and tubes having large cross-sections, because the sample is heated from the inside.

Our previous paper[2] presented the details of physical changes for a series of relatively thin POM tapes drawn by the MISELA method in the draw ratio range of 10 to 30. This paper concerns the morphological changes of a POM rod with a large cross-section during drawing, and describes the sonic modulus change in the furnace, the deformation mechanism and crystalline orientation in the necking zone, and the orientation behaviour at the advanced ultra-drawing stage.

EXPERIMENTAL

Sample preparation and drawing method

The material used was as described in our previous paper[2]. A POM rod with a diameter of 6.4 mm was drawn continuously by the MISELA method.

The MISELA apparatus is composed of a feeder, a microwave heating furnace and a take-up machine. The microwave heating furnace is 6.6 m in length and includes waveguides for microwave heating, matching waveguides and dummy roads. To draw the POM rod effectively, the ambient temperature of the inside of all waveguides is controlled by electronic heaters mounted around these waveguides[3].

The POM rod was drawn at a 20:1 draw ratio. The rod in the course of the drawing process was taken out of the drawing furnace for analysis just after the stable drawing procedure was stopped.

The draw ratio (λ) of the POM rod during drawing was determined using the following equation:

$$\lambda = (D_0/D_L)^2 \tag{1}$$

where D_0 is the original POM rod diameter and D_L is the diameter during drawing at a distance of L from the furnace entrance.

Sonic modulus

The rod diameter decreases continuously during drawing. Therefore, it is impossible to measure the Young modulus of the rod by tensile test or dynamic mechanical measurement because its diameter changes. Young's moduli were determined by measuring the sonic pulse propagation time, which is independent of sample diameter. The sonic modulus[4] (E_s) is expressed by the following equation:

$$E_s = \rho V^2 \tag{2}$$

where ρ (1.42 g cm^{-3}) is the density of the sample and V is the sonic velocity. The measurement of sonic modulus was carried out at room temperature. The pulse frequency was 10 kHz and the pulse propagation length was 10 cm.

Orientations and thermal properties

Wide-angle X-ray diffraction (WAXD) patterns were taken by an X-ray diffractometer using a Laue camera. The azimuthal intensity distribution of the (100) plane reflection of a POM crystal was measured by the diffractometer using a fibre specimen holder. The azimuthal scan was done from $-90°$ to $+90°$. The X-ray source used was Ni-filtered 40 kV/20 mA CuKα radiation focused by a 1 mm diameter collimator.

0032-3861/85/121929-06$03.00

Birefringence of microtomed samples ~20 μm thick was determined based on the optical retardation measured by a beam with a diameter of 100 μm. The birefringence change with draw ratio was determined by the average value of the birefringence distribution in the radial direction.

Change in thermal properties was also investigated by the differential scanning calorimetry (d.s.c.) method. The details of WAXD, birefringence and d.s.c. methods have been described elsewhere[2,5].

RESULTS AND DISCUSSION

Change in the modulus during drawing

Figure 1 shows changes in the rod diameter and sonic modulus (E_s) of the POM rod in the necking region. The necking occurs from $L=0.25$ m. During necking formation, the diameter decreases and E_s increases drastically. *Figure 2* shows changes in the diameter and E_s throughout the whole drawing process. The broken curve shows an ideal change in rod diameter (D_c) under the optimum drawing condition[6]. The diameter decreases more drastically than D_c in the first half of advanced ultra-drawing and more gradually than D_c in the latter half. The drastic diameter decrease in the first half region may be due to the higher microwave field power adopted experimentally than under the optimum drawing condition[6]. A detailed study is given in the last section. Plateaux on the diameter curves, in which E_s is also kept unchanged, are observed both after necking and on the final drawing stage. The levelling-off is thought to be caused by the change in microwave heating power, since the plateaux coincide with matching waveguide positions. *Figure 3* shows the change in E_s with draw ratio, replotted from *Figure 2*. This linear increase in E_s is also observed[2] for POM tapes drawn at draw ratios of 10–29.

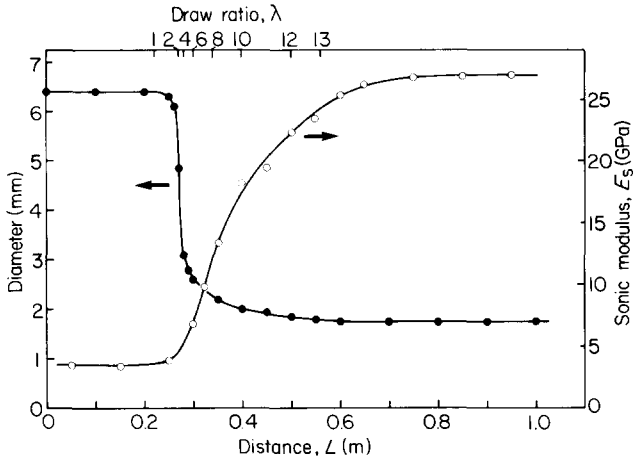

Figure 1 POM rod diameter and sonic modulus (E_s) vs. distance (L) from the furnace entrance end in the necking region

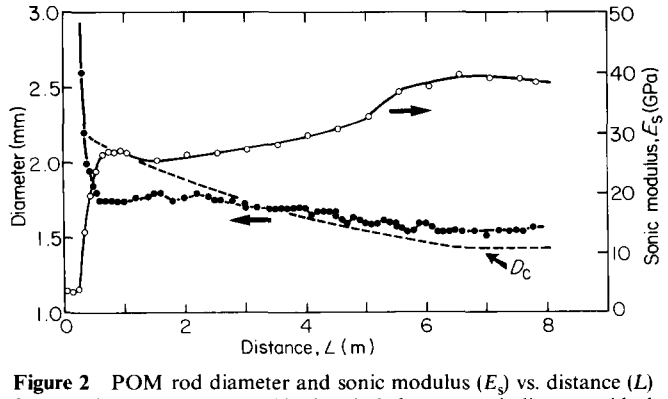

Figure 2 POM rod diameter and sonic modulus (E_s) vs. distance (L) from the furnace entrance end in the whole furnace. D_c indicates an ideal diameter change under the optimum conditions[6]

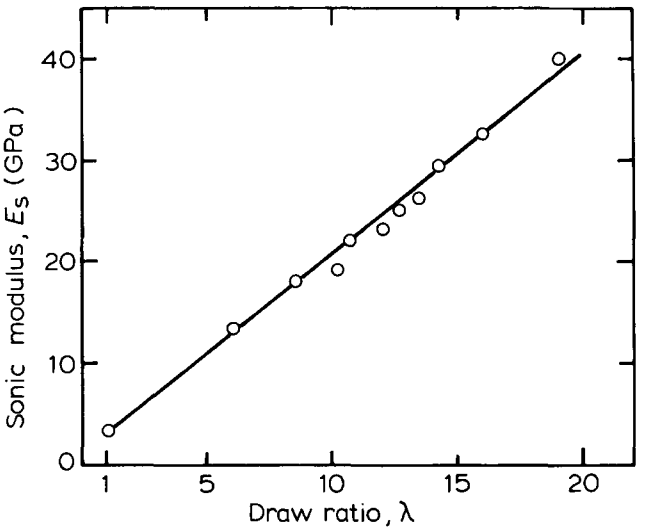

Figure 3 Sonic modulus (E_s) vs. draw ratio (λ)

Deformation mechanism in the necking zone

Figure 4 shows the WAXD pattern change of POM rod in the necking region. The inner and outer rings are formed by the (100) and (115) planes of the POM crystal, respectively. *Figure 4* indicates that an abrupt crystalline orientation developed in the necking region. *Figure 5* shows the change in the azimuthal reflection patterns of the (100) plane in the necking region. Intensities at $\alpha=0$ and $+90°$ (or $-90°$) indicate crystalline orientations parallel and perpendicular to the draw direction, respectively. Here, α indicates an azimuthal angle of the (100) plane diffraction. At the first stage of necking ($L=0.26$–0.265 m), a weak peak appears at $\alpha=90°$. The peak at $\alpha=90°$ is due to crystalline orientation perpendicular to the draw direction. At the next stage ($L=0.27$ m), a peak at $\alpha=0°$ is also observed, together with the peak at $\alpha=90°$. At the following stage ($L=0.275$–0.28 m), the peak at $\alpha=0°$ grows drastically and the peak at $\alpha=90°$ almost vanishes. Finally, the peak at $\alpha=0°$ becomes sharper ($L=0.30$ m). This sharp peak at $\alpha=0°$ is due to the high degree of crystalline orientation parallel to the drawing direction.

The unexpected crystalline orientation perpendicular to the draw direction appears only in the early stage of the necking region and is different from the stable perpendicular orientation of polypropylene fibre[7,8]. The perpendicular orientation of POM in the necking region is related to the deformation mechanism on necking. The large plastic deformation mechanism on drawing for crystalline polymers can be classified into three forms[9]: (1) unfolding, (2) block fracturing and (3) tilting. In deformation by tilting, lamellae of a crystalline polymer orient at 45° inclination[10] to the draw direction during plastic deformation. In deformation by block fracturing, lamellae are fractured into small crystalline regions with rotation to the draw direction. Therefore, in these two deformation mechanisms, molecular chains do not orient themselves perpendicular to the draw direction. On the other hand, in

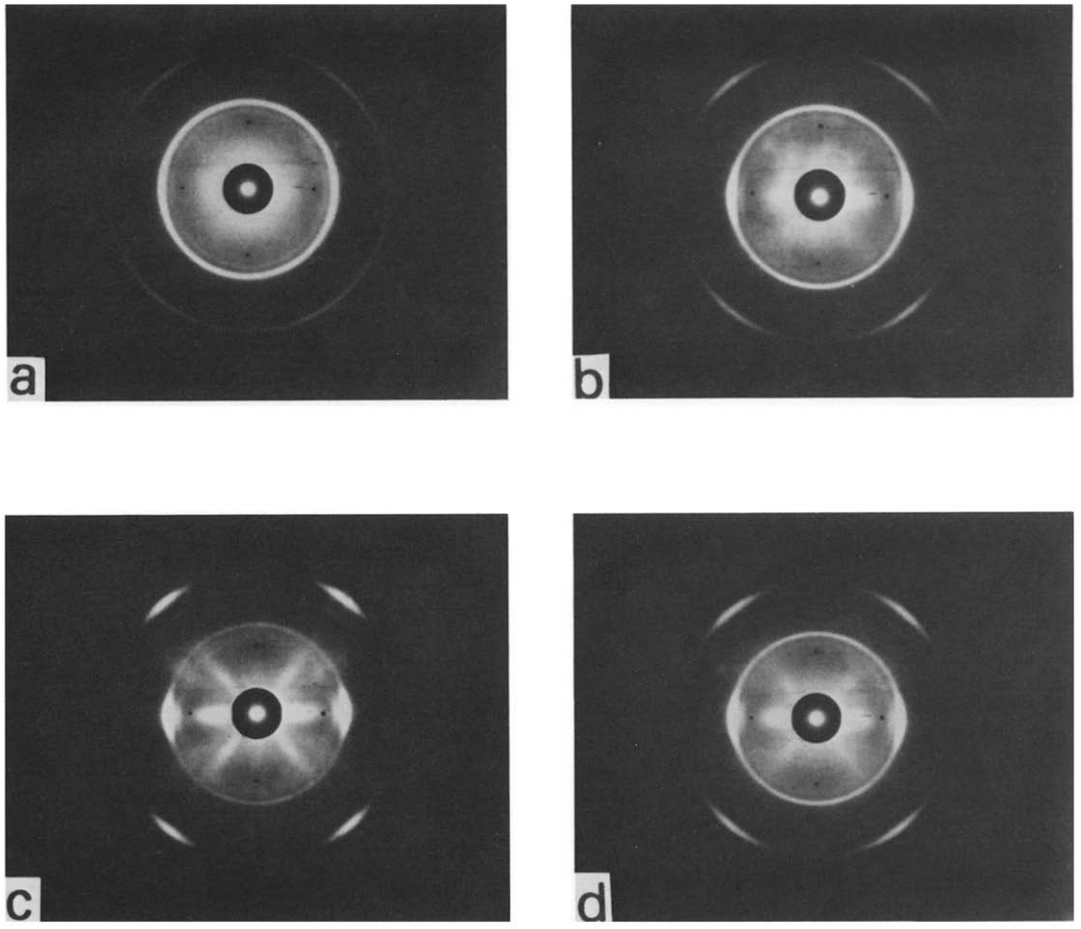

Figure 4 Wide-angle X-ray diffraction pattern change of a POM rod in the necking zone for different values of L: (a) 0.264 m; (b) 0.267 m; (c) 0.27 m; (d) 0.275 m

the unfolding of molecular chains, lamellae rotate perpendicular to the draw direction. Therefore, the X-ray diffraction analyses show that, on necking of POM rods, lamellae rotate perpendicular to the draw direction and then are unfolded in the draw direction.

Crystalline orientation in necking region

Figure 6 shows the change in crystalline orientation function with draw ratio calculated using the azimuthal distribution of the (100) reflection (*Figure 5*). The value of the crystalline orientation function increases abruptly with necking deformation and reaches 0.988 at relatively low draw ratio of ~ 6. This value is almost equal to the maximum value (0.99) finally obtained[2]. That is, the crystalline regions of the rod orient fully to the draw direction immediately after necking.

Figure 7 shows the draw ratio dependence of average birefringence. Birefringence is not observed until the draw ratio reaches 2 ($L \simeq 0.27$ m), although plastic deformation has already occurred. WAXD results show the presence of molecular chains perpendicular to the draw direction even in the range of less than $L = 0.27$ m. Therefore, the fact that no birefringence is observed for draw ratio of less than 2 is considered to be due to the compensating effect of molecular orientations parallel and perpendicular to the draw direction with each other. It is clear from *Figures 6* and *7* that an abrupt increase in birefringence in the draw ratio range of 2–6 is due to crystalline orientation to the draw direction. The tensile deformation in the first step ($L = 0.25$–0.30 m) is accompanied by overall morphological change.

Orientation behaviour in the advanced ultra-drawing stage

The second step corresponds to a draw ratio range greater than 6 ($L > 0.30$ m). The increase in Young's modulus in this step is due to increases in both volume fraction crystallinity and amorphous orientation. Since these changes are not accompanied by whole plastic deformation, the increases in crystalline orientation and birefringence are not so large (*Figures 6* and *7*). *Figure 8* shows changes in Young's modulus (E_a) at amorphous regions during drawing. Here, E_a values were evaluated by assuming a simple series structure model[11]. The volume fraction crystallinity used was estimated from the ratio of heat of fusion to that of POM crystal (75.3 cal g^{-1})[12]. The E_a value in the first step remains almost unchanged, whereas the increases in crystalline orientation function and birefringence are remarkable. This result indicates that the tensile stress in the first step mainly applies to crystalline orientation due to lamellar unfolding. On the

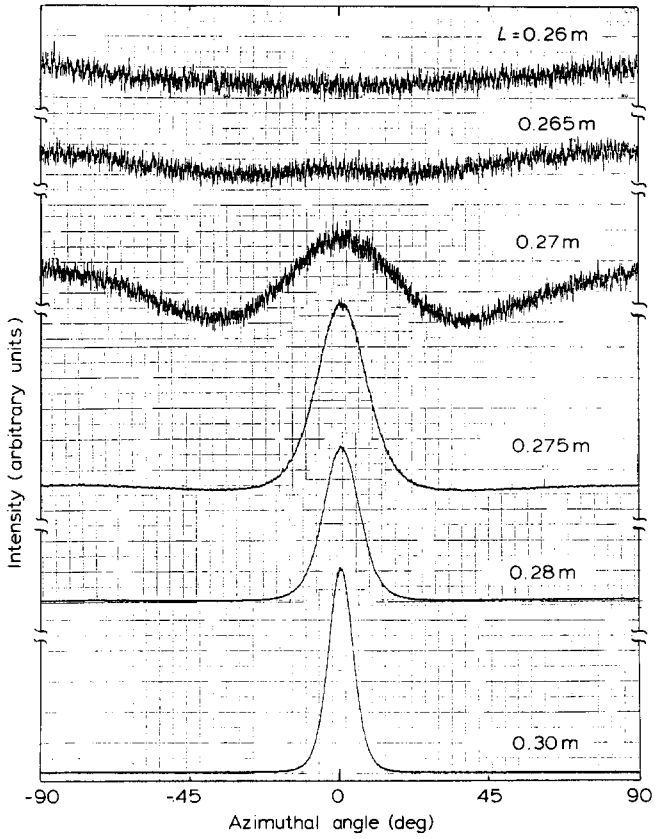

Figure 5 The change in azimuthal reflection patterns of (100) plane with distance (L) from the furnace entrance end

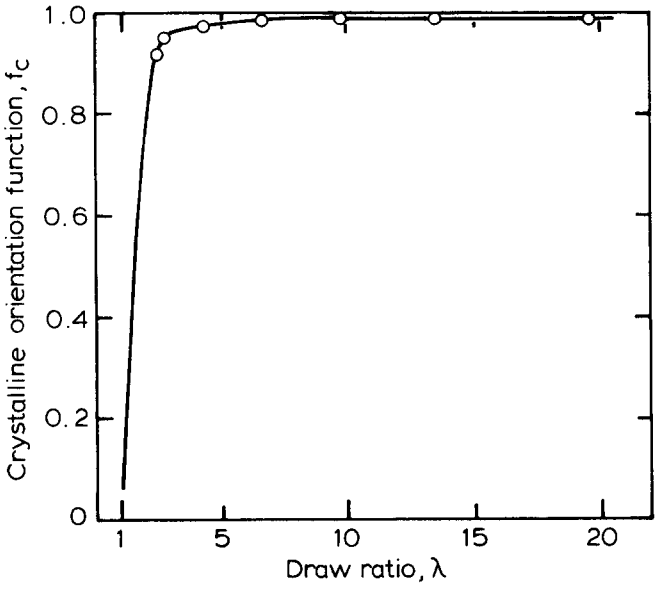

Figure 6 Crystalline orientation function (f_c) vs. draw ratio (λ)

other hand, in the second step, the tensile stress can be considered to apply effectively to amorphous orientation (or taut-tie molecular formation) because there is no further change in crystalline regions.

In the second step, the Young modulus (E_s) of the POM rod increases from 15 to 40 GPa. This increase is as large as ~60% of the final value. In addition, amorphous modulus (E_a) increases from 3 to 18 with increasing draw ratio. It can be concluded that ultra-high moduli are attained by amorphous orientation during the advanced ultra-drawing process.

Orientation distribution in the radial direction

Figure 9 shows the birefringence distribution change in the radial direction during drawing. Birefringence in the necking region is homogeneous with the radial direction. In the range of $L > 0.30$ m, however, birefringence inside of the oriented POM rod is depressed but not that outside. *Figure 10* shows the d.s.c. heating thermograms of the oriented POM rod. The peak on the outside of the rod reaches a high temperature during drawing and becomes sharp. This indicates that crystalline regions grow uniformly in length during drawing. On the other hand, another small peak at a lower temperature is observed in the d.s.c. curve inside of the rod at $L \geqslant 0.385$ m. This small peak does not change during drawing, although the higher peak gradually moves to higher temperatures. The temperature of this lower peak is nearly equal to that of the original rod. These results indicate that relaxation of crystalline orientation occurred partially inside of the rod, depressing the increase in birefringence as a result.

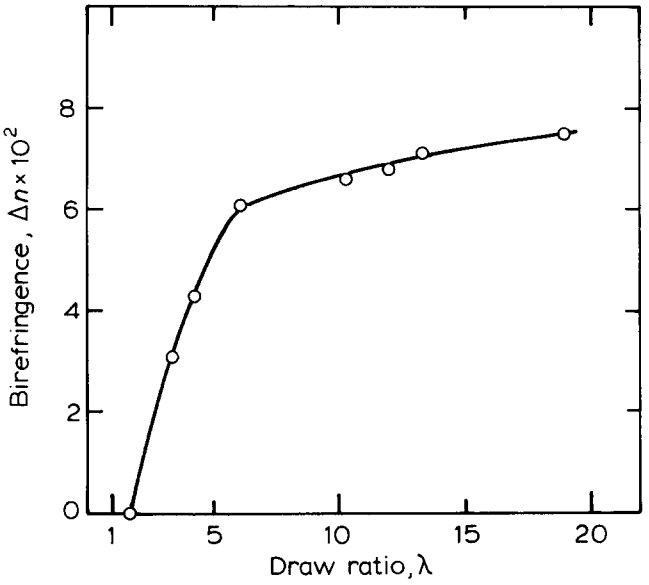

Figure 7 Average birefringence (Δn) vs. draw ratio (λ)

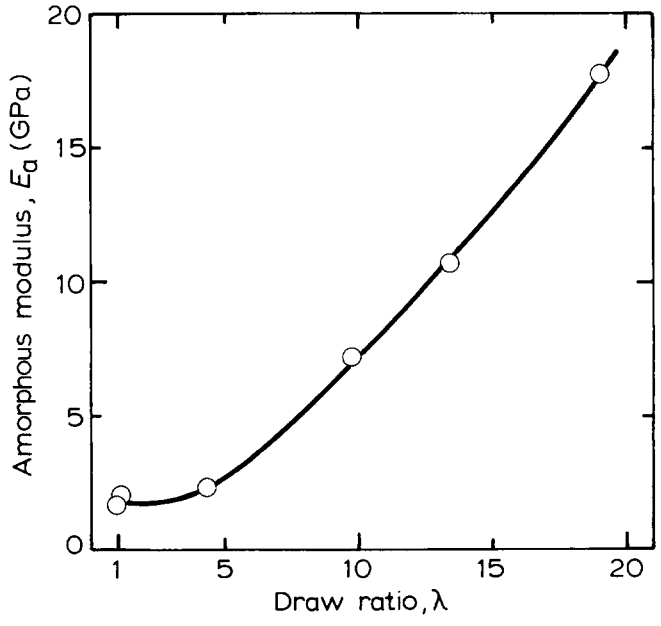

Figure 8 Amorphous modulus (E_a) vs. draw ratio (λ)

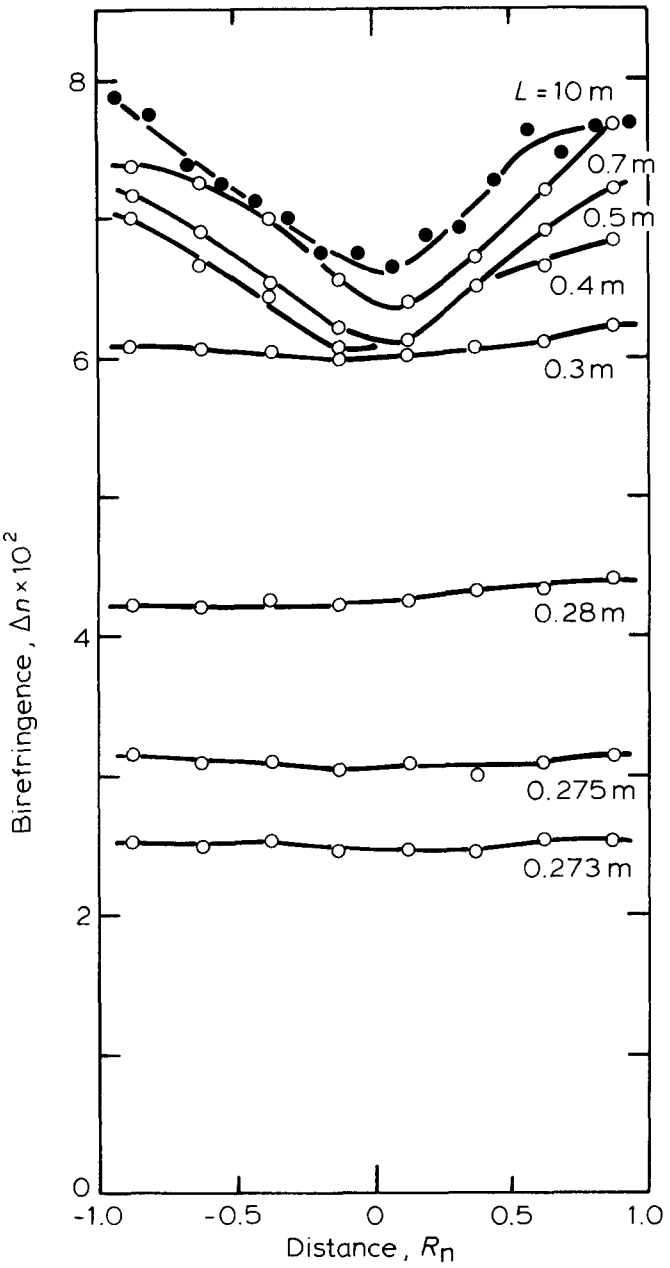

Figure 9 Birefringence (Δn) distribution change in the radial direction with distance (L) from the furnace entrance end. R_n indicates normalized distance from the rod centre

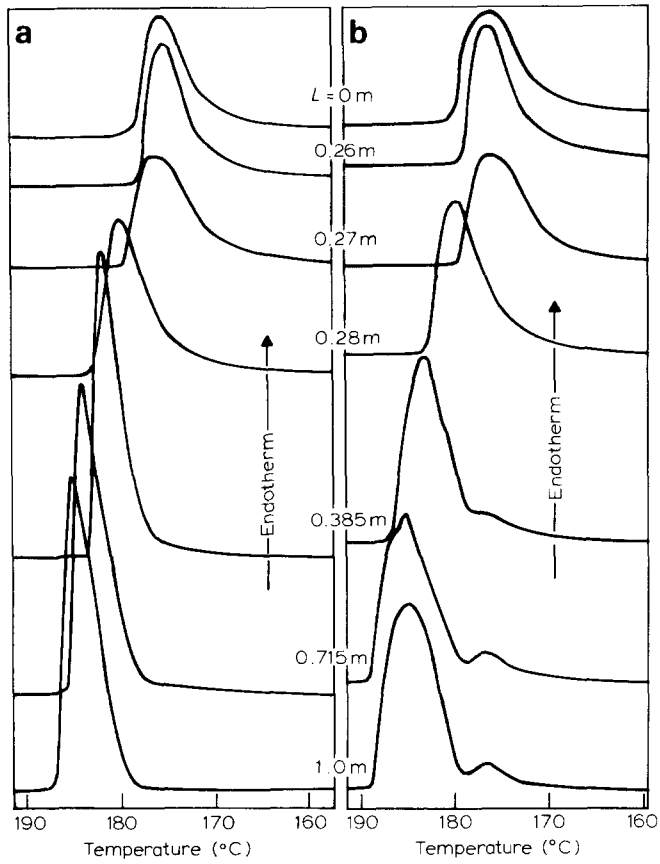

Figure 10 The d.s.c. heating thermogram changes (a) outside and (b) inside of the POM rod with distance (L) from the furnace entrance end

During the microwave heating drawing, the POM rod is heated from the inside and heat emission occurs from the surface. Therefore, it is likely that the temperature inside of the rod becomes higher than that near the surface, if the rod is not drawn under the optimum drawing condition. In this case, the birefringence value should gradually become lower towards the inside of the rod. This situation seems to correspond to the actual one confirmed experimentally, as was also predicted from the difference between changes both in the actual rod diameter and in the optimum one (D_c) (*Figure 2*). It should be noted that fine adjustments of ambient temperature and microwave power are required to get ultra-high-modulus POM rods over 40 GPa with large cross-sections.

CONCLUSION

The increase in Young's modulus during a microwave heating drawing process was, similarly to drawn POM, simply related to the attenuation of cross-sectional area even in the necking region. Lamellae rotated perpendicular to the draw direction and were unfolded into fibrils during plastic deformation in the necking region. Crystalline regions fully oriented to the draw direction immediately after the necking at a draw ratio of 6. The Young modulus reached 15 GPa with necking. An ultra-high modulus over 15 GPa was attained by amorphous orientation in the advanced ultra-drawing stage and reached 40 GPa at a final draw ratio of 20. In this stage, the relaxation of crystalline orientation occurred inside of the rod because of little heat emission.

ACKNOWLEDGEMENTS

The authors wish to thank Nobuo Inagaki and Shinzo Yamakawa for their continuous encouragement. They also thank Tsuneo Konaka for useful discussions throughout the course of this work.

REFERENCES

1 Nakagawa, K., Maeda, O. and Yamakawa, S. *J. Polym. Sci., Polym. Lett. Edn.* 1983, **12**, 933
2 Takeuchi, Y., Yamamoto, F. and Nakagawa, K. *J. Polym. Sci., Polym. Phys. Edn.* in press

3 Nakagawa, K., Konaka, T. and Yamakawa, S. *Polymer* 1985, **26**, 84
4 Ward, I. M. 'Structure and Properties of Oriented Polymers', Applied Science, London, 1975
5 Konaka, T., Nakagawa, K. and Yamakawa, S. *Polymer* 1985, **26**, 462
6 Nakagawa, K., Konaka, T. and Yamakawa, S. *Polym. Prep. Jpn.* 1983, **32**(10), 2997
7 Awaya, H. *J. Chem. Soc. Jpn., Pure Chem. Sect.* 1961, **82**, 1575
8 Ishizuka, O., Matsumura, S., Kobayashi, K. and Horio, M. *J. Chem. Soc. Jpn., Indust. Chem. Sect.* 1962, **65**, 990
9 Iida, S. 'Mechanical Properties 2' (in Japanese), Kyouritsu, Tokyo, 1983, p. 346
10 Peterlin, A. and Sakaoku, K. *J. Appl. Phys.* 1967, **38**(11), 4152
11 Takeuchi, Y., Yamamoto, F. and Nakagawa, K. *J. Polym. Sci., Polym. Lett. Edn.* 1984, **22**, 159
12 Iguchi, M. *Makromol. Chem.* 1976, **177**, 549